ORIGINAL RESEARCH

GALE Promotes the Proliferation and Migration of Glioblastoma Cells and Is Regulated by miR-let-7i-5p

Xiaopeng Sun [1,2]
Hao Xue [1,3]
Ye Xiong [4]
Rui Yu [5]
Xiao Gao [1]
Mingyu Qian [1]
Shaobo Wang [1]
Huizhi Wang [1]
Jianye Xu [1]
Zihang Chen [1]
Lin Deng [1,3]
Gang Li [1,3]

[1]Department of Neurosurgery, Qilu Hospital of Shandong University, Jinan, Shandong Province 250012, People's Republic of China; [2]Department of Neurosurgery, Dezhou People's Hospital, Dezhou, Shandong Province 253014, People's Republic of China; [3]Institute of Brain and Brain-Inspired Science, Shandong Provincial Key Laboratory of Brain Function Remodeling, Shandong University, Jinan, Shandong Province, People's Republic of China; [4]Department of Neurosurgery, First Affiliated Hospital of Wenzhou Medical University, Wenzhou, Zhejiang Province 325000, People's Republic of China; [5]Department of Neurosurgery, The Second Hospital of Shandong University, Jinan 250033, People's Republic of China

Purpose: Glioma is the most common and lethal type of brain tumor. While GALE (UDP-galactose-4-epimerase) has been shown to be overexpressed in some kinds of cancers, its expression in gliomas has not been reported. MicroRNAs (miRNAs) function as tumor suppressors in many cancers, and online datasets can be used to predict whether GALE is regulated by miR-let-7i-5p. In this investigation, we explored the effect and regulatory mechanisms of GALE on glioblastoma growth via miR-let-7i-5p.

Methods: We used a Cox proportional hazards model and publicly available datasets to examine the relationship between GALE and the survival rates of glioma patients. Bioinformatics predicted the targeting of GALE by miR-let-7i-5p. The proliferation, migration, cell cycle and apoptosis of human glioblastoma cells were assessed by relevant assays. We also demonstrated the effect of GALE on glioblastoma multiforme [GBM] tumor growth using an in vivo orthotopic xenograft model.

Results: GALE was upregulated in human gliomas, especially in high-grade gliomas (e.g., GBM). An obvious decline in GALE expression was observed in human glioblastoma cell lines (U87 and U251) following treatment with a small interfering RNA (siRNA) targeting GALE or miR-let-7i-5p mimics. Knockdown of GALE or overexpression of miR-let-7i-5p (with miR-let-7i-5p mimics) inhibited U87 and U251 cell growth. miR-let-7i-5p significantly restrained the migration ability of human glioblastoma cells in vascular mimic (VM), wound healing and transwell assays, and GALE promoted glioblastoma growth in vivo.

Conclusion: Our findings confirm that GALE plays an important role in promoting the development of human glioma and that GALE can be regulated by miR-let-7i-5p to inhibit human glioblastoma growth.

Implications for cancer survivors: Our data show that cancer survivors have low GALE expression, which indicates that GALE may be a diagnostic biomarker and a promising therapeutic target in glioblastoma.

Keywords: glioblastoma, GALE, miR-let-7i-5p, proliferation, migration

Introduction

Glioblastoma, as the most malignant type of human glioma, is one of the most deadly tumor types in humans. Despite substantial advances in imaging diagnosis, surgery, chemotherapy, and radiation therapy, glioma patients do not have an ideal prognosis.[1] According to the World Health Organization (WHO) classification, gliomas are divided into four grades (I-IV). Glioblastoma (WHO grade IV) leads to the worst prognosis, with a median survival time of only 12 to 15 months after a confirmed diagnosis.[2,3]

Correspondence: Gang Li; Lin Deng
Department of Neurosurgery, Qilu Hospital of Shandong University, Jinan, Shandong Province 250012, People's Republic of China
Email ligangqiluhospital@163.com; denglinqilu@163.com

UDP-galactose-4-epimerase (GALE), a key enzyme of galactose metabolism,[4,5] is overexpressed in some kinds of cancers, such as papillary thyroid carcinoma,[6] and we also found GALE overexpression in glioblastoma. We used a dual-luciferase gene reporter assay to confirm whether miR-let-7i-5p directly inhibits GALE expression, which would result in the subsequent inhibition of glioblastoma multiforme (GBM) cell proliferation and migration.

MicroRNAs (miRNAs) constitute a class of single-stranded noncoding RNA that are approximately 20 to 22 nucleotides (nt) in length and have been shown to inhibit gene expression at the posttranscriptional level.[7] miRNAs have been confirmed to play important roles in cell development,[8–10] progression[11,12] and human cancer recurrence.[13] Mutations in let-7, which was first discovered in *Caenorhabditis elegans*, can lead to abnormal larval growth and are therefore lethal to these organisms.[14] Bioinformatics analysis has demonstrated that the microRNA let-7 is highly conserved in various animal species, supporting its important role in early developmental stages.[14,15] Let-7 plays a vital role in the cell cycle and polarization. The expression of a few miR-let-7 family members has been discovered in many malignancies, including pancreatic cancer,[16] human colon cancer,[17] human lung cancers[18] and breast cancer.[19] However, the association of miR-let-7i-5p with glioma progression remains unknown. In this study, the specific functions of miR-let7i-5p in human GBM were explored in multiple GBM cell lines.

In the current research, we examined GALE in human glioma to elucidate its association with tumor progression, and our findings reveal the tumor-suppressive effect of GALE regulated by miR-let-7i-5p for GBM therapies.

Materials and Methods
Cox Proportional Hazards Model

We used the Cox proportional hazards model to identify genes that are associated with patient survival and to build a model for future predictions. The outcome was defined as disease-free survival (in months). N genes were selected to construct the Cox regression model; for each gene Gj (j=1, 2, …, N), we built the following Cox model for the hazard of vital status or death at time t,

$$\lambda_j(t) = \lambda_{0j}(t)\exp\left(\alpha_j G_j + \beta_1 X_1 + \ldots + \beta_p X_p\right)$$

$$= \lambda_{0j}(t)\exp(\alpha_j G_j + \beta' X)$$

where $\lambda_{0j}(t)$ is the baseline hazard function for gene Gj, and X1, X2, …, XP are covariates. The covariates that we adjusted for included race, age, sex, Karnofsky performance score (KPS), tumor status, and history of neoadjuvant treatment. Using the method described above, GALE was selected.

Tissue Samples and Databases

The human glioma samples and normal brain tissues utilized in this study were provided by the Department of Neurosurgery at the Qilu Hospital of Shandong University. The protocol was approved by the hospital, and informed consent was obtained in writing from each patient. Tissue samples, including 4 normal brain tissues, 4 WHO grade I tissues, 8 WHO grade II tissues, 7 WHO grade III tissues and 9 WHO grade IV (GBM) tissues, were obtained from the patients by routine surgical treatment. Several experienced clinicopathologists classified glioma specimens according to the WHO tumor classification criteria. The Cancer Genome Atlas (TCGA) database (n = 667; http://cancergenome.nih.gov) was utilized in this study (Table 1).

Cell Culture and Reagents

The human glioblastoma cell lines U87 and U251 were purchased from the Cell Bank of the Chinese Academy of Sciences and cultured in Dulbecco's Modified Eagle's

Table 1 Correlation of GALE Expression in Human Glioma Patients with Multiple Clinicopathological Features. *P* Values Were Acquired by Chi-Square and Fisher's Precise Tests

Variable		GALE High Expression	GALE Low Expression	*p* value
Age	≥45	263	241	<0.05
	<45	83	109	
Gender	Male	200	198	0.776
	Female	146	151	
KPS	≥80	150	156	<0.05
	<80	47	22	
WHO grade	II	57	160	<0.001
	III	107	130	
	IV	135	19	
IDH status	Mutant	137	285	<0.001
	Wild-type	180	51	
MGMT promoter	Methylated	180	292	<0.001
	Unmethylated	114	47	
1p/19q	Codeletion	12	156	<0.001
	Non-codeletion	309	183	

Medium (DMEM) containing 10% fetal bovine serum (FBS) at 37°C in a 5% CO_2 incubator.

Cell Transfection

A small interfering RNA (siRNA) against GALE (referred to as si-GALE), a mature miR-let7i-5p mimic, a miR-let7i-5p inhibitor and a negative control (NC) duplex were designed and provided by GenePharma (Shanghai, China). When the cells became 70% confluent, they were transfected or cotransfected with Lipofectamine 3000 (Invitrogen, Carlsbad, CA, USA) according to the manufacturer's instructions. Quantitative real-time PCR was used to verify the transfection efficiency. After transfection for 48 h, glioma cells were collected for subsequent experiments.

Cell Viability Assay

U251 and U87 cells were inoculated into 96-well cell culture plates at a density of 3000 cells/well, and cell proliferation was analyzed at 24, 48, and 72 h after transfection with a Cell Counting Kit-8 (CCK-8) assay. Briefly, 10 μL of CCK-8 solution was added to each well, and the plate was incubated in a humidified atmosphere for an additional hour. Then, EnSight (PerkinElmer) was used to measure the optical density at 450 nm. The DNA synthesis of glioma cells transfected with the si-GALE, miR-Let7i-5p or NC constructs in the 24-well culture plate was detected with an EdU Apollo 567 In Vitro Kit (Cell-Light). A Leica DMI 8 microscope was used to visualize the EdU results.

Vascular Mimic (VM) Formation Assay

VM formation assays were carried out according to the previously described experimental methods. In short, a 96-well cell culture plate was coated with Matrigel Basement Membrane Matrix (50 μL/well, BD Bioscience), which was allowed to polymerize at 37°C for 30 mins. In total, 2×10^4 cells/mL (100 μL/well) were suspended on the matrix, incubated in DMEM supplemented with 1% FBS at 37°C and 5% CO_2 for 24 h and examined under an inverted microscope.

Wound Healing Assay

Cells (1×10^5) were inoculated into 6-well plates overnight and transfected with the si-GALE, miR-Let7i-5p or NC construct. When the cells reached 90% confluence, the tip of a sterile pipette was used to scratch the cell layer, and the freed cells were washed away with phosphate-buffered saline (PBS). Scratched plates were cultured in DMEM containing 1% FBS. Changes were observed under a Leica microscope, and images along the scratch line were acquired at 0 to 12 h. The relative scratch width was defined according to the offset distance from the original scratch distance.

Cell Migration Assays

Cell migration was analyzed using a transwell chamber with a diameter of 6.5 mm (8 μm pore size, Corning). In FBS-free medium, a total of 5×10^4 transfected cells were inoculated into the upper chamber of an uncoated transwell incubator. Culture medium containing 10% FBS was added to the lower chamber. After 12, 24 and 48 h, the nonmigrating cells were removed with cotton buds. The cells transferred to the lower surface were fixed, stained with crystal violet for 15 mins, and counted under a microscope in five random fields.

Bioinformatics Prediction and Luciferase Reporter Assay

GALE correlation analysis was performed for the gene expression profile available in The Cancer Genome Atlas (TCGA) dataset. Multiobjective prediction programs, including the online miRNA prediction tools TargetScan human 7.2 and miRBase, were used to identify common miR-let-7i-5p targets predicted by computer-aided algorithms. The miR-let-7i-5p-GALE and miR-let-7i-5p-mutGALE (target seed sequence with a mutation) reporters were constructed by BioSune (Jinan, China). Glioma cells were coinfected with a luciferase reporter and test material or a vector using Liposome 3000. After 48 h of transfection, cellular luciferase activity was analyzed using a Dual-Luciferase Reporter Assay Kit (Promega) according to the manufacturer's protocol. Firefly luciferase activity was normalized to that of Renilla luciferase.

RNA Extraction and Real-Time Quantitative PCR

According to the manufacturer's instructions, total RNA was extracted using TRIzol reagent and then reverse transcribed into cDNA using miRNA stem-loop RT primers or U6 RT primers and a ReverTra Ace qPCR RT Kit. Real-time PCR was performed with an SYBR Premix Ex Taq™ Kit, and the primers are shown in Table 2. A LightCycler® 480 II instrument was used for the amplification reactions, and the expression levels of U6 and GAPDH were used as endogenous controls. The Roche LightCycler ® 480 II

Table 2 Oligonucleotide Sequences

Name[a]	Sequence (5′ to 3′)[b]
miR-let-7i-5p mimics (sense)	UGAGGUAGUAGUUUGUGCUGUU
NC (sense)	UUCUCCGAACUGGUCACGUTT
si-GALE (sense)	CCCUGAAUGUCUUUGGCAATT
U6-F	TGCGGGTGCTCGCTTCGGCAGC
GALE-F	AAATGATCCGGGACCTGTGC
GALE-R	ATCGCCACCTGGGAGACATA
GAPDH-F	GCACCGTCAAGGCTGAGAAC
GAPDH-R	TGGTGAAGACGCCAGTGGA
Homo-GALE (let7i)-wild	GAGCTCGGACCCTCCCCTACCAAGGACCAGGAAAAGCAGCAGCTGCCTGCTCTCCAGCCTCTGGCAGG AACTCAGGGCCCTGGAGCTGCTGGGGCCAAGCCAAGGCCTCCC*CTACCTCA*AACCCCAGCTGGGCCCG CTTAGCCCACCAGGCATGAGGCCAAGGGCTCCACTGACCAGGAGGCCGAGGTCTCTAACTCTTATCTTC CACAGGGTCCAAGAGTTCATCAGGACCCCCAAGAGTGAGTGAGGGGGCAAGGCTCTGGCACAAAACCT CCTCCTCCCAGGCACTCATTTATATTGCTCTGAAAGAGCTTTCGCTAGC
Homo-GALE (let7i)-mut	GAGCTCGGACCCTCCCCTACCAAGGACCAGGAAAAGCAGCAGCTGCCTGCTCTCCAGCCTCTGGCAGG AACTCAGGGCCCTGGAGCTGCTGGGGCCAAGCCAAGGCCTCCCGGAGGGGTAACCCCAGCTGGGCCC GCTTAGCCCACCAGGCATGAGGCCAAGGGCTCCACTGACCAGGAGGCCGAGGTCTCTAACTCTTATCTT CCACAGGGTCCAAGAGTTCATCAGGACCCCCAAGAGTGAGTGAGGGGGCAAGGCTCTGGCACAAAACC TCCTCCTCCCAGGCACTCATTTATATTGCTCTGAAAGAGCTTTCGCTAGC

Notes: [a]F, forward primer; R, reverse primer. [b]Target sites are in bold and italics; mutated target sites are underlined.

system was used to calculate the expression level for the concentration ratio.

Western Blot Analysis

Total protein was extracted with RIPA buffer containing 1% benzoyl fluoride, and equal amounts of protein were loaded onto a 10% SDS polyacrylamide gel. Next, the samples were incubated with primary antibodies overnight at 4°C and then with the appropriate secondary antibody conjugated to horseradish peroxidase for 1 h at room temperature. Finally, ChemiDoc XRS + (BIO-RAD) was used to visualize the protein bands, and laboratory imaging software was used for detection. The relative comprehensive density was determined by comparing the expression levels of β-actin to those of GALE (1:5000, Abcam) and other related proteins.

Immunohistochemical (IHC) Staining

Human glioma tissue specimens or solid tumors harvested from mice were fixed with 4% formaldehyde. Paraffin-embedded tumor sections at up to 5-μm thickness were fixed on positively charged microscope slides, and antigen was recovered with 1 mM EDTA. The endogenous

peroxidase activity was quenched by incubating the slides in methanol containing 3% hydrogen peroxide, and the slides were then washed in PBS for 6 mins. Then, the slide was incubated with normal goat serum for 2 hrs at room temperature and then with the appropriate antibody at 4°C. Then, the sections were rinsed with PBS, incubated with horseradish peroxidase-conjugated goat anti-rabbit or anti-mouse antibodies, reacted with diaminobenzidine and restained with hematoxylin.

Flow Cytometry Assay

Cell cycle distribution and apoptosis were measured by flow cytometry. For cell cycle analysis, the tryptophan method was adopted. Briefly, transfected glioma cells were collected by washing three times with cold PBS, incubating with 70% ethanol overnight at 4°C, washing with PBS in the dark at room temperature and incubating with propidium iodide for 15 mins in the dark. Finally, the cells were analyzed by a FACScan flow cytometer (BD, USA).

According to the manufacturer's instructions, an Invitrogen Life Technologies (CA) kit was used to analyze cell apoptosis. The transfected cells were collected and incubated with V-FITC and propidium iodide (PI) at

room temperature in the dark for 15 mins. These cells were then analyzed by flow cytometry (BD). Each experiment was carried out three times.

Orthotopic Xenograft Glioma Mouse Model

In the in vivo study, luciferase-labeled U87 cells (1×10^6 cells per mouse) were implanted into the brains of BALB/c nude male mice (Jiangsu Jicuiyaokang Biotechnology Co., LTD., Nanjing, China) at the age of 4 weeks in a three-dimensional manner to yield intracranial tumor xenografts. According to the standard protocol, cultured luciferase-labeled U87 cells were infected with the LV3-GALE-home-899 or LV3-NC lentivirus vector (Shanghai General Pharmaceutical). Mice were randomly divided into two groups (NC and sh-GALE), with five mice in each group. The animals were imaged with a PerkinElmer IVIS system every 5 days. According to the code of ethics, when the final images were significantly different between the two groups on day 20, the mice were sacrificed. After sacrifice, the entire brain was removed, fixed with 4% paraformaldehyde, dehydrated, and embedded in paraffin wax. Continuous slices at 5 μm thickness were cut, stained with hematoxylin and eosin (H&E), and evaluated under a microscope. The mice were treated and tested according to the Animal Research: Reporting In Vivo Experiments Guidelines (ARRIVE Guidelines). The experiment was approved by the Animal Management and Use Committee of Shandong University.

Statistical Analysis

All experiments were carried out in triplicate. SPSS 22.0 and GraphPad Prism software were used to perform statistical analyses and generate experimental graphs. Descriptive statistical methods, including the mean ± standard deviation, student's t-tests, Kaplan–Meier diagrams, logarithmic rank tests, one-way analysis of variance and Spearman correlation tests, were used to analyze significant differences. *$P<0.05$, *$P<0.01$ and ***$P<0.001$ were considered statistically significant.

Results

GALE Expression Is Associated with a High Tumor Grade in Gliomas

To investigate the role of GALE in glioma development, we first analyzed GALE gene expression levels in normal brain tissues in the GBM, low-grade glioma (LGG) and TCGA datasets. Compared with normal, LGG and TCGA

brain tissues, GBM tissues had significantly higher GALE mRNA levels (Figure 1A). GALE protein levels were detected by immunohistochemistry in a separate cohort of human glioma (n=32) and normal brain (n=4) tissues from Qilu Hospital (Jinan, China). Consistent with the mRNA expression results, GALE protein expression in GBM tissues was higher than that in LGG or normal brain tissues (Figure 1D). Therefore, GALE was positively associated with a high tumor grade in both the public database and our primary tumor sample cohort.

GALE Expression Is Associated with a Poor Prognosis

A Kaplan-Meier survival curve was used to analyze the prognostic value of GALE expression for the overall survival (OS) of glioma patients. Compared with LGG ($P<0.001$) and GBM ($P<0.05$) patients in the TCGA (n=667), patients with high GALE expression had a significantly worse prognosis (Figure 1B and C). Therefore, GALE may be a new biomarker for the prognosis of glioma.

Silencing GALE Decreases the Proliferation and Migration of Glioma Cells in vitro

To directly detect the effects of GALE on the survival and proliferation of glioma cells, GALE was inhibited by siRNA induction (Figure 2A and B), and CCK-8 and EdU assays were performed. Downregulation of GALE resulted in significantly decreased percentages of OD450- and EdU-positive U87 and U251 cells at 48 h after transfection (Figure 2C–F). To further determine whether GALE had an effect on cell growth, a colony-forming assay was used to evaluate cell proliferation. Notably, GBM cell lines showed significant clonogenic inhibition in the siRNA treatment group (Figure 2G), suggesting that GALE regulates the proliferation of GBM cells.

VM, wound healing and perforation assays were used to observe the effect of GALE on the migration of GBM cells. U87 and U251 cells were treated with NC or si-GALE. Compared with the NC group, the si-GALE group showed less simulated vascular formation, less effective wound closure and fewer stained cells in the VM, wound healing and transwell assays (Figure 3). These results show that the knockdown of GALE significantly inhibited the migration ability of GBM cell lines. Next, we used Western blot analysis to study the downstream targets of GALE. GALE gene knockout significantly reduced the
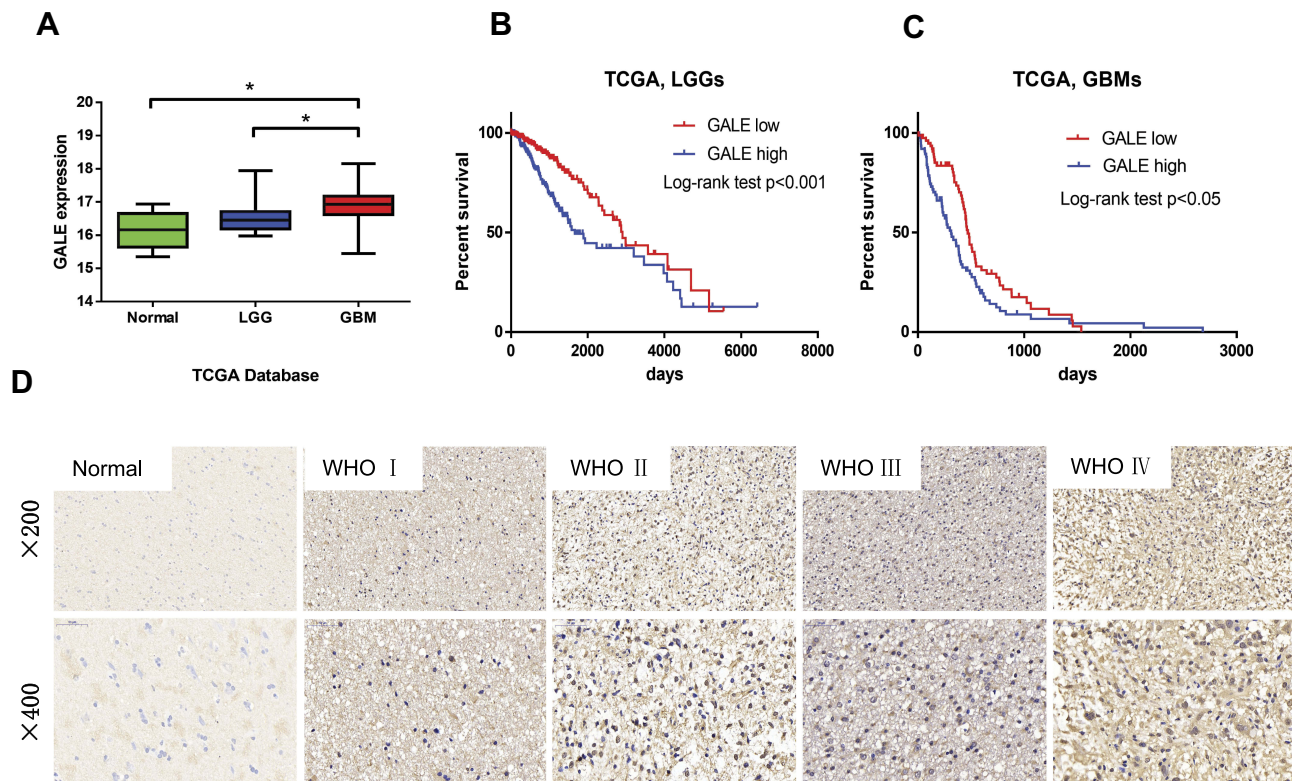
Figure 1 GALE expression in glioma is associated with tumor grade. (**A**) Quantitative analysis of GALE gene expression in the TCGA dataset. (**B, C**) The prognostic significance of GALE expression in LGG and GBM patients in the TCGA (n=667) database was analyzed. (**D**) IHC staining of GALE expression in gliomas of different grades and normal brain specimens. Magnification: ×200, upper; ×400, lower. *P < 0.05.

levels of N-CAD, MMP-2, and several genes/pathways critical for the progression of various types of cancer, including glioma (Figure 4H and I).

Human Glioma Cell Cycle Arrest and Apoptosis Induced by GALE Knockdown

Cell cycle analysis by flow cytometry also showed that GALE knockdown increased the number of U87 and U251 cells in the G1 phase (Figure 4A–C). In addition, in U87 and U251 cells, silencing GALE promoted apoptotic cell death compared with that in the corresponding control (Figure 4D and E). In Western blot analysis, the expression levels of cyclin-dependent kinase 2 (CDK2), CDK4, cyclin A2 and BCL-2 were decreased after GALE silencing. In contrast, the bax and cleaved caspase-3 expression levels were increased in the si-GALE group (Figure 4F and G). In summary, these results suggest that the absence of GALE inhibits the progression of the glioma cell cycle and induces the apoptosis of glioma cells.

miR-Let-7i-5p Directly Targets GALE

It is generally believed that miRNAs perform posttranscriptional regulation by binding to the 3′-untranslated regions (UTRs) of their target genes. To examine the effect of GALE on cell migration and invasion, we used the bioinformatics prediction software TargetScan (http://www.targetscan.org/) to identify its targets. Among thousands of candidates, we focused on miR-let-7i-5p. To determine whether miR-let-7i-5p regulates cell migration and invasion through the 3′-UTR of GALE, we conducted a luciferase reporter assay on U251 glioma cells (Figure 5A). In miR-let-7i-5p-transfected cells, luciferase activity was decreased by approximately 76.8% relative to that of cells transfected with control miRNA. To determine the inhibitory effect of miR-let-7i-5p at the protein level, after the addition of the miR-let-7i-5p inhibitor and stimulation of U251 and U87 cells, we observed significantly lower GALE protein levels in stimulated U251 and U87 cells than in miRNA-transfected glioma cells in the NC.

GALE Is Involved in the miR-let-7i-5p-Induced Repression of GBM Cell Proliferation and Migration

To explore whether miR-let-7i-5p has functions similar to those of GALE in GBM cells, an RNA approach
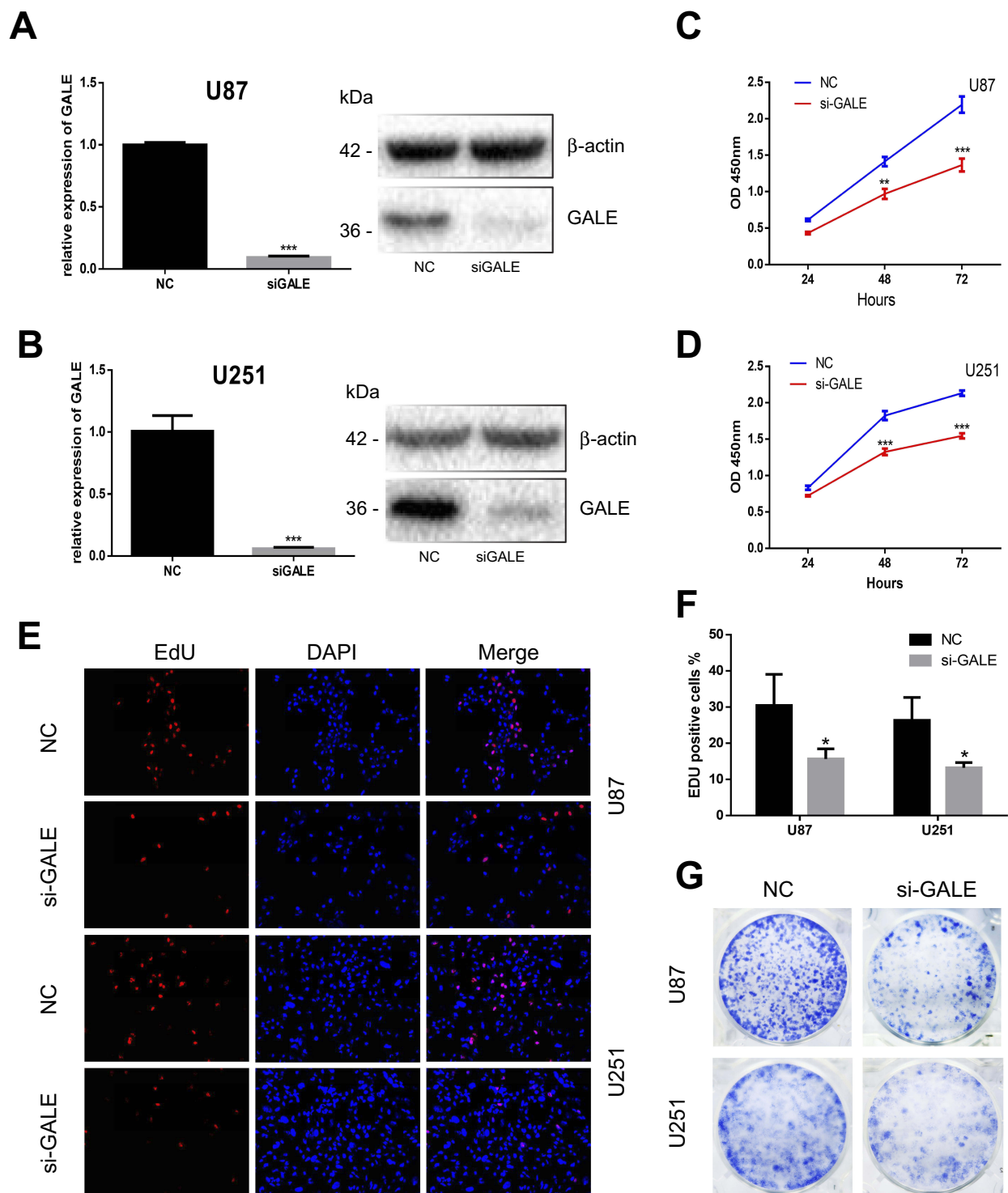
Figure 2 Silencing GALE reduces the proliferation of glioma cells. (**A, B**) Quantitative real-time PCR analysis showed that the relative mRNA level of GALE after si-GALE transfection was significantly decreased. GAPDH was used as the control. Western blot analysis of U87 and U251 cell lysates transfected with NC and GALE siRNAs and incubated with the GALE antibody. β-Actin was used as the control. (**C, D**) Growth curves of U87 and U251 cells based on the absorbance at OD_{450}. (**E, F**) The transfection was followed by EdU analysis 48 h later. (**G**) The clonal formation of glioblastoma cells was decreased after si-GALE therapy. *$P < 0.05$; **$P < 0.01$; ***$P < 0.001$.

was used. The overexpression of miR-let-7i-5p was confirmed by real-time RT-PCR and Western blot analysis (Figure 5B–E). After overexpressing miR-let-7i-5p, we performed EdU and colony formation assays on the U87 and U251 cell lines, and significant differences in the results of both assays were observed between the miR-let-7i-5p overexpression and NC groups (Figure 6A–C).
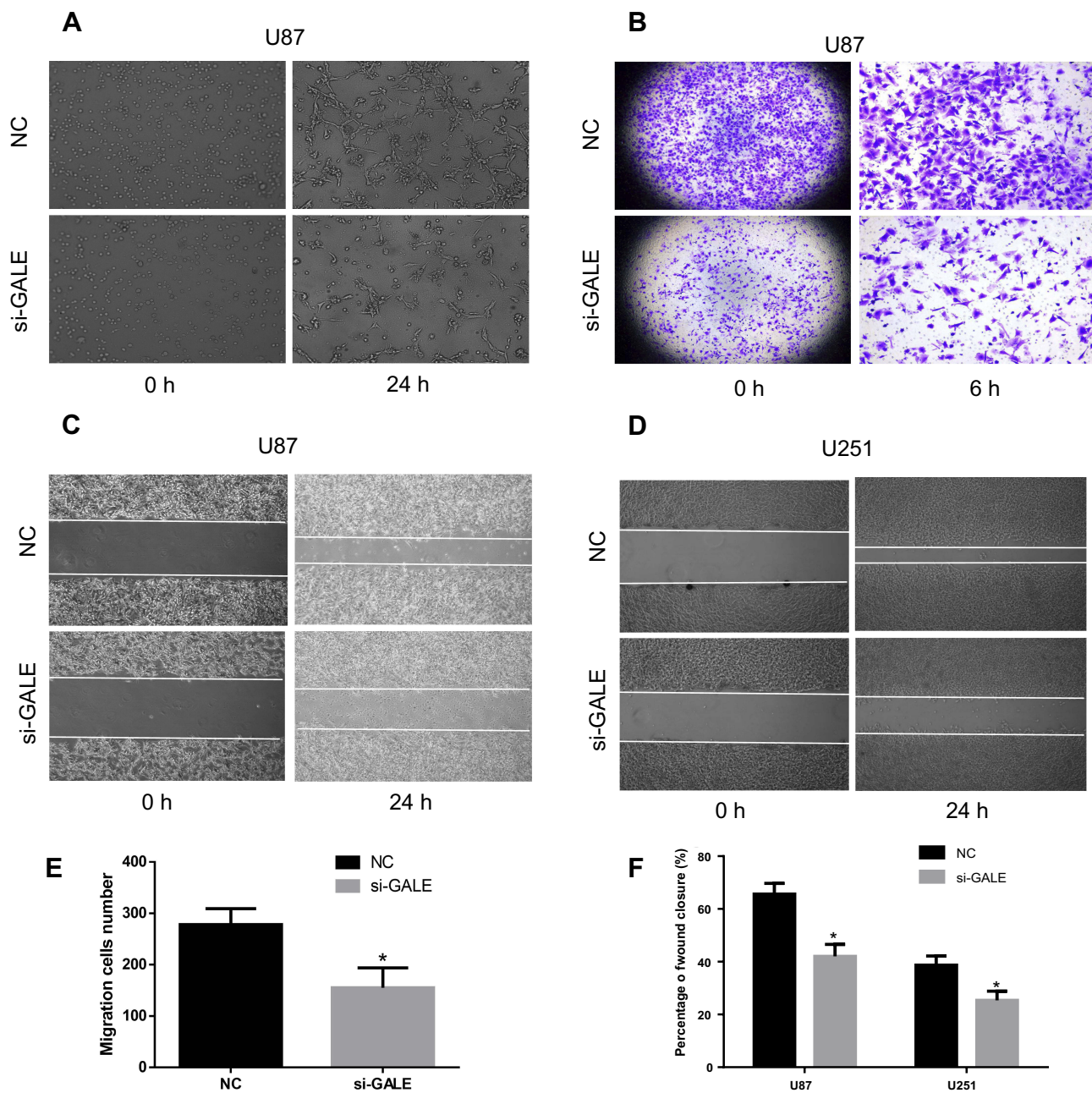
Figure 3 Silencing GALE reduces the migration of glioma cells. (**A**) A 24-h VM formation assay was performed in U87 cells. (**B, E**) U87 cells were transfected with NC or si-GALE. Cell migration was assessed 6 h after culture by transwell analysis. (**C, D, F**) U87 and U251 cells were transfected with NC or si-GALE and analyzed for wound healing during the 24-h recovery period. *P < 0.05.

Then, VM, wound healing and transwell assays were performed to elucidate the role of miR-let-7i-5p in the migration of GBM cells. Both U87 and U251 cells were treated with miR-let-7i-5p mimics. Compared with the NC group, the miR-let-7i-5p mimic group showed delayed wound closure and fewer stained cells in the VM, wound healing and transwell assays (Figure 7). Western blot analysis also showed results similar to those of the si-GALE group (Figure 6D). These results suggest that overexpression of miR-let-7i-5p leads to

significant inhibition of migration, similar to that observed following GALE silencing.

Silencing GALE Inhibits Tumorigenesis in vivo

To further investigate the effect of the GALE protein on human glioma, we evaluated tumor growth in vivo. Luciferase-labeled U87 glioma cells were transfected with a lentivirus construct
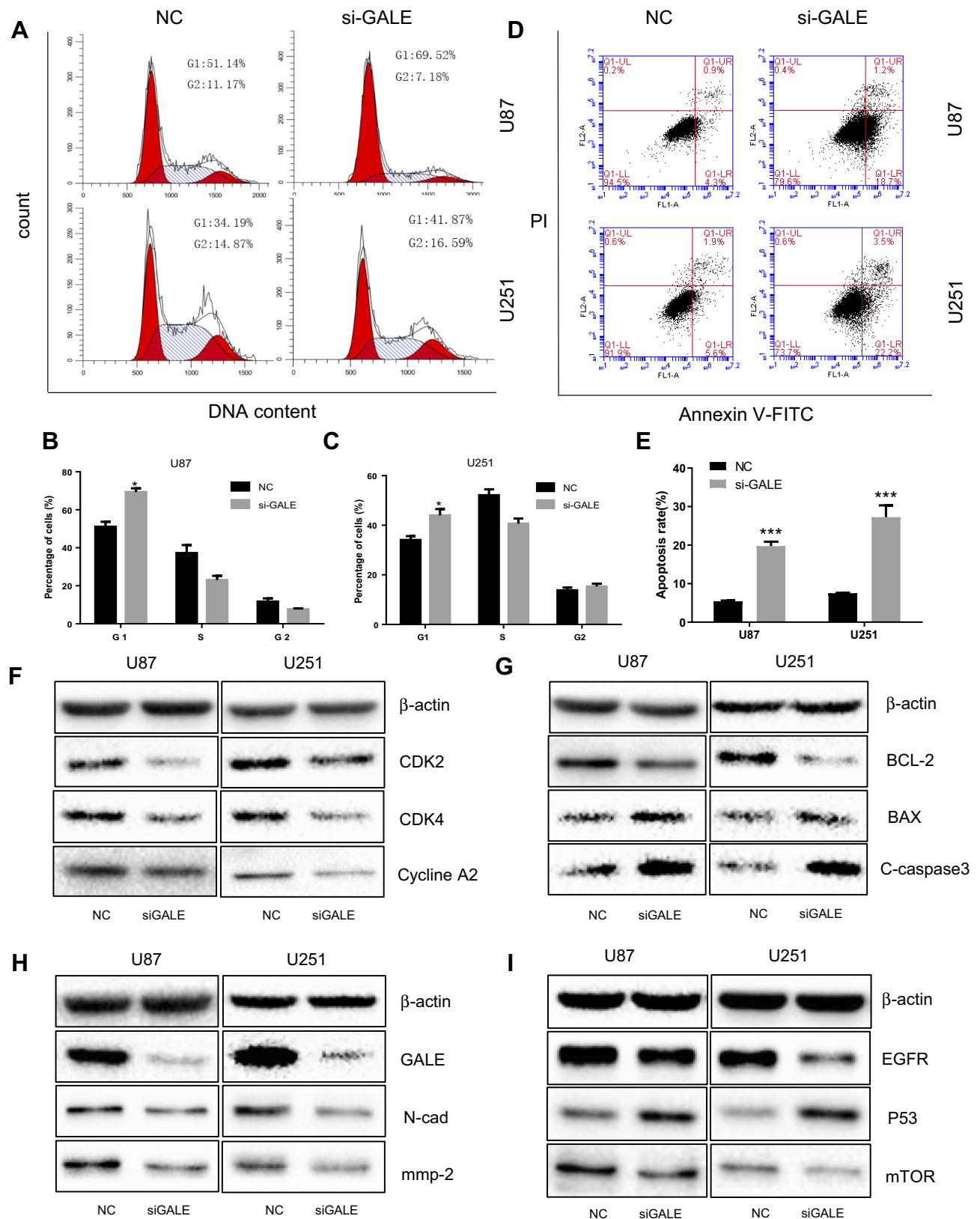
Figure 4 Knockdown of GALE induces cell cycle arrest and apoptosis in human glioma cells. (**A–C**) U87 and U251 cells were transfected with NC or si-GALE and then subjected to cell cycle analysis by flow cytometry. Three independent experiments were carried out in each group. (**D, E**) Flow cytometry was used to detect the apoptosis rate of cells using the membrane protein V-FITC antibody and PI staining. (**F–I**) Western blot analysis of the expression levels of known cell cycle regulators, cell apoptosis markers, epithelial–mesenchymal transition (EMT) markers and possible cell signaling pathway proteins. *P < 0.05; ***P < 0.001.
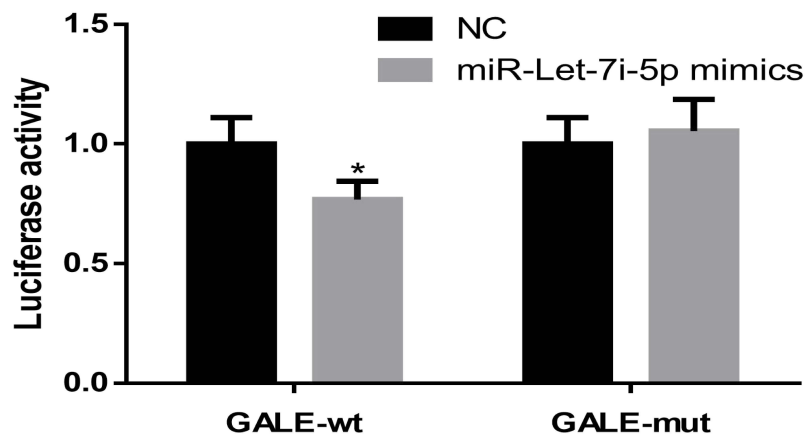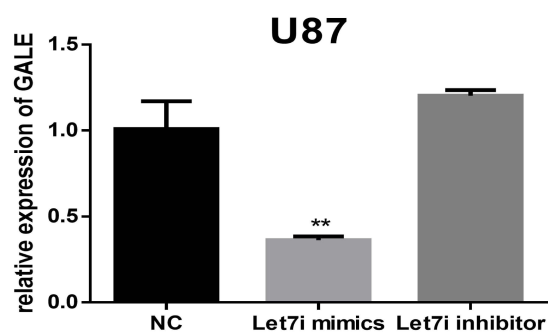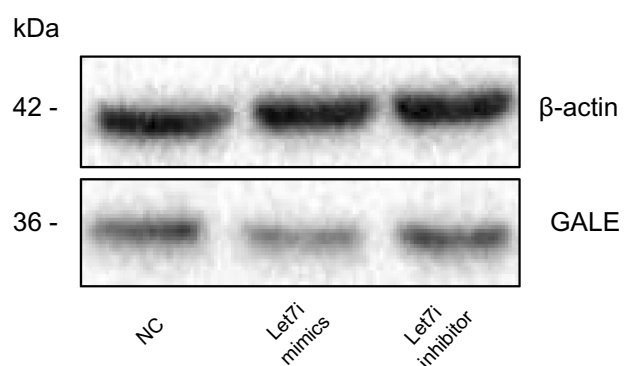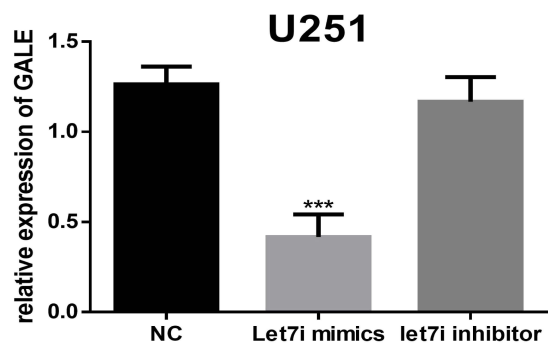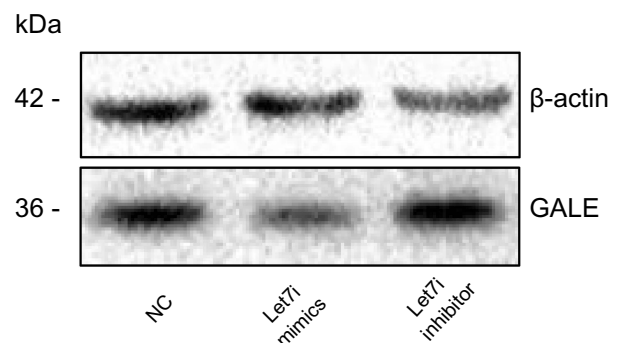
Figure 5 Mir-let-7i-5p directly targets GALE. Sequence of the miR-let-7i-5p binding site and luciferase analysis of the GALE 3′-UTR. Bioinformatics was used to predict the miR-let-7i-5p binding site in the 3′-UTR of GALE. (**A**) A 3′-UTR vector was cotransfected with miR-let-7i-5p or NC miRNA into U251 cells. Relative luciferase activity was measured in the cytolytic solution 48 h after transfection. Luciferase activity levels were compared with those of NC miRNA-transfected cells, which were normalized to 1. (**B–E**) Quantitative real-time PCR analysis showed that the relative mRNA level of GALE after simulated transfection with miR-let-7i-5p was significantly decreased. GAPDH was used as the control. After miR-let-7i-5p mimics were transfected, GALE expression was confirmed by Western blot analysis. β-Actin was used as the control. *P < 0.05; **P < 0.01; ***P < 0.001.
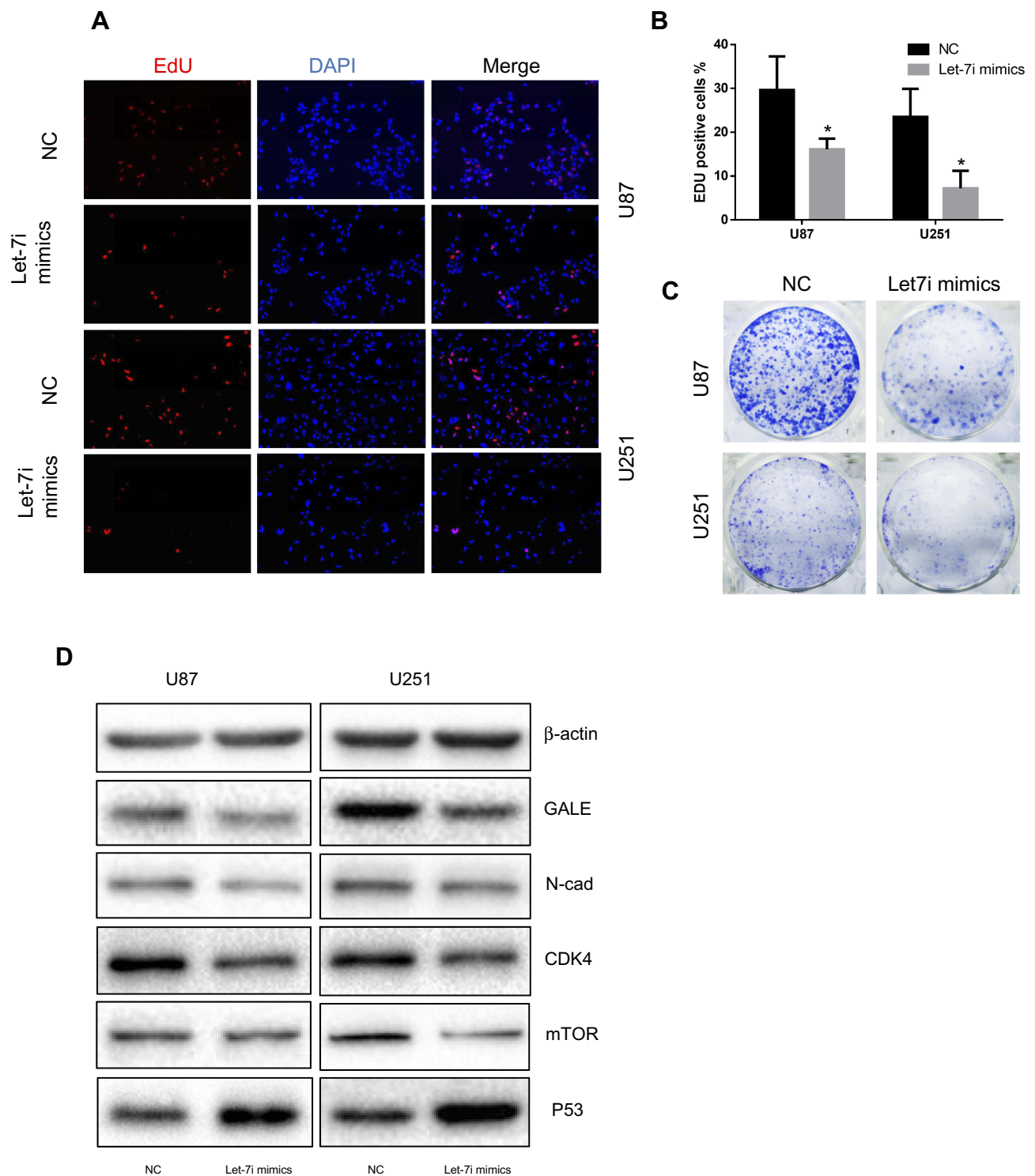
Figure 6 Overexpression of miR-let-7i-5p reduces the proliferation of glioma cells. (**A, B**) EdU assays performed 48 h after transfection. (**C**) The clonogenicity of glioblastoma cells treated with miR-let-7i-5p mimics was decreased. (**D**) The expression levels of EMT markers, cell cycle regulatory factors, and other possible cell signaling pathway proteins were compared between the NC and miR-let-7i-5p mimic groups by Western blot analysis. *P < 0.05.

expressing a GALE-targeted small hairpin RNA (shRNA) or a control shRNA. An in situ xenograft was established by implanting sh-GALE or NC cells into nude mice. Bioluminescence imaging (BLI) systems were used weekly to evaluate tumor development in each group. Compared with mice in the control group, animals in the sh-GALE group showed a significantly reduced tumor size (Figure 8A and B), more limited boundaries (Figure 8C), and increased
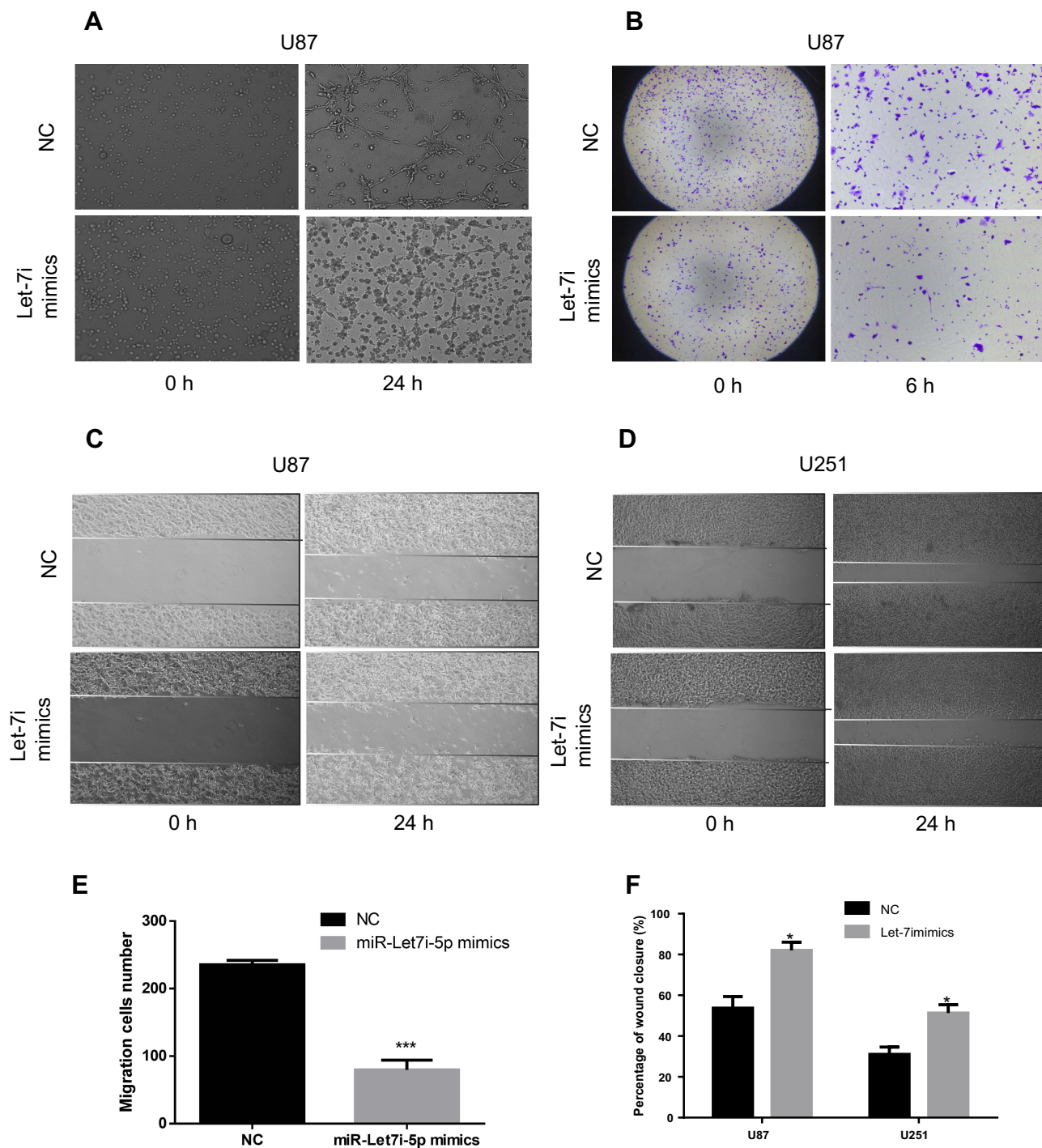
Figure 7 Overexpression of miR-let-7i-5p reduces the migration of glioma cells. (**A**) A VM formation assay of U87 cells was performed for 24 h. (**B, E**) U87 cells were transfected with the NC or miR-let-7i-5p mimics. Cell migration was assessed 6 h after culture by transwell analysis. (**C, D, F**) U87 and U251 cells were transfected with the NC or miR-let-7i-5p mimics, and wound healing assays were performed during the 24-h recovery period. *P < 0.05; ***P < 0.001.

survival (Figure 8D). Immunohistochemistry confirmed a reduction in GALE protein levels in xenografts produced by sh-GALE cells. Bcl-2, MMP-2 and the proliferation index

marker ki-67 were also reduced in xenografts (Figure 8E–I). These results suggest that GALE knockdown results in the reduced growth and invasion of glioma cells in the body.
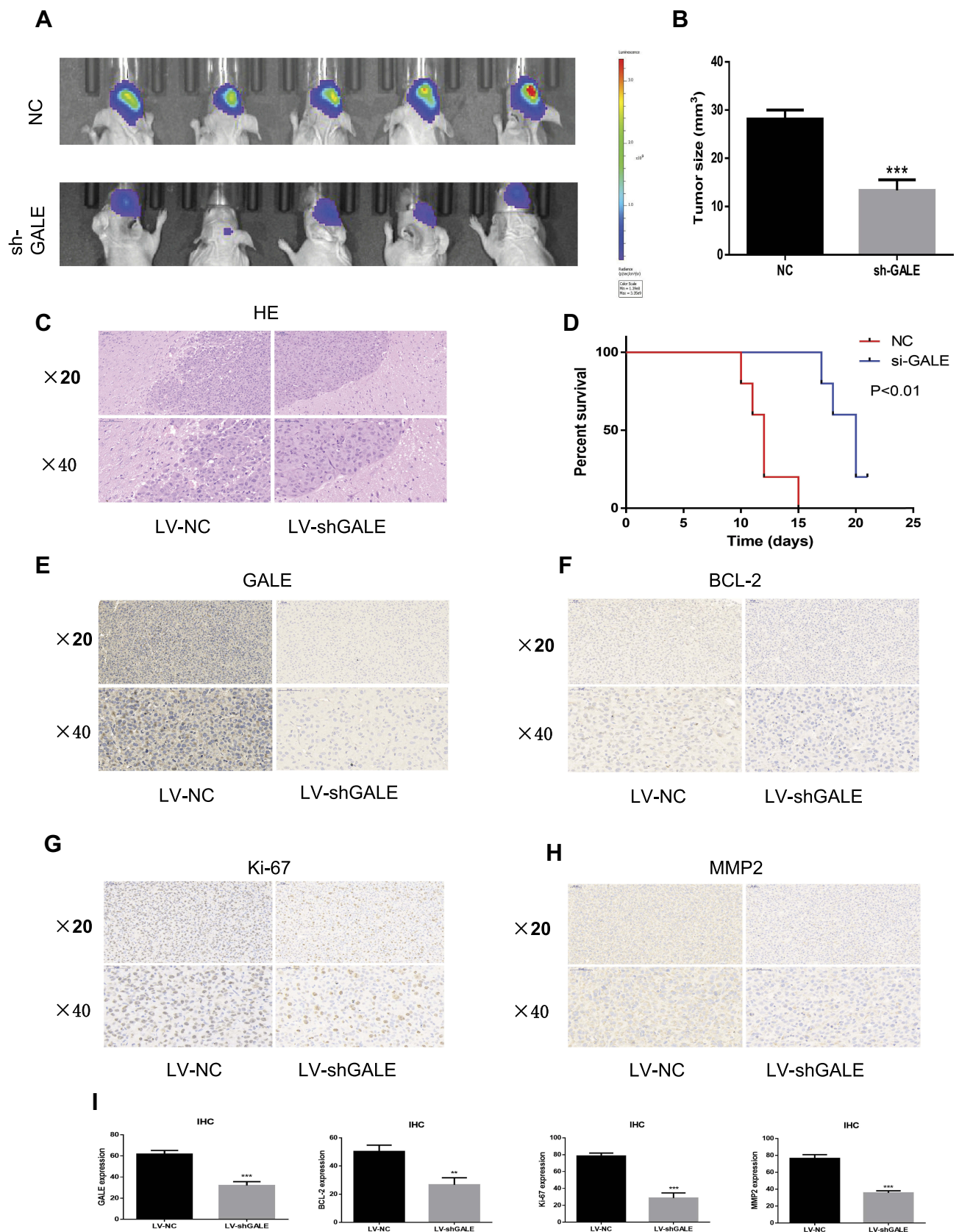
Figure 8 Silencing GALE inhibits tumorigenesis in vivo. (**A**) A BALB/c nude mouse model of orthotopic xenograft glioma tumor development in each group was evaluated by a bioluminescence imaging (BLI) system. (**B**) The tumor size (mm^3) was measured. (**C**) Brain sections from mouse xenografts comprised of 3×10^5 U87 NC or sh-GALE cells were stained with H&E. (**D**) Survival rate analysis of animals implanted with cells expressing U87 NC or sh-GALE (log-rank test P<0.01; 5 animals in each group). (**E–I**) IHC analysis of GALE, BCL-2, Ki-67 and MMP2 in sections from the indicated xenografts. Magnification: ×200 and ×400. **P < 0.01; ***P < 0.001.

Discussion

While human glioma has been sufficiently characterized at the molecular level, the significance of changes in the expression levels of numerous genes is not attributable to any underlying biological function. Here, we studied the function of GALE, a gene that is highly expressed in GBM compared to LGG, and high GALE expression was associated with a poor prognosis in glioma patients.

Abnormal cell proliferation and growth are characteristics of human glioma. Many genetic changes lead to uncontrolled growth through the maladjustment of proteins directly involved in cell cycle progression and apoptosis.[20]

GALE is a bifunctional enzyme that catalyzes the reversible conversion of DP-galactose (UDP-Gal) to UDP-glucose (UDP-Glc) as part of the Leloir pathway of galactose metabolism[2] and the formation of UDP-N-acetylgalactosamine (UDP-GalNAc) from UDP-N-acetylglucosamine (UDP-GlcNAc) in the presence of NAD+, an essential step in generating sugar moieties for glycoprotein synthesis.[3,21–23]

GALE is dynamically regulated in various metabolic settings.[24–29] Defects in the conversion of UDP-galactose to UDP-glucose have been reported to result in common characteristics of galactosemia, including vomiting, hypotension, epileptic seizures, jaundice, galactosuria, and hepatomegaly.[30,31] A deficiency in GALE or low GALE enzyme activity leads to mild clinical symptoms of galactosemia.[32]

GALE gene knockout reduced cell proliferation and migration in vitro and in vivo, induced G1 cell cycle arrest, promoted cell apoptosis, and reduced the growth of in situ xenotransplantation. These results suggest that GALE is a potential molecular target for GBM therapy.[33] In addition, to reveal the potential molecular mechanism by which GALE promotes glioma development, we evaluated whether GALE expression changes regulate key genes or pathways in cancer progression, such as N-cad, MMP-2, P53, CDK2, CDK4 and BCL-2.

An increasing number of small tumor-suppressive miRNAs have been found, including miR-637,[34] miR-663,[35] miR-218,[36] miR-128[37] and miR-34a.[38] Many studies have reported a direct relationship between let-7 expression and cell differentiation. On the other hand, their lack of expression is associated with a variety of invasive cancers. Here, we identified miR-let-7i-5p as a novel tumor-suppressive miRNA.

We used the online miRNA prediction tool TargetScanHuman 7.2 to identify miR-let-7i-5p target gene sequences in the 3′-UTR of GALE mRNA. Next, double luciferase analysis was performed, revealing that the luciferase activity in miR-let-7i-5p-transfected cells was significantly lower than that in the control group. In addition, GALE protein levels were significantly reduced in miR-let-7i-5p mimic-transfected U251 and U87 cells. These results suggest that GALE is a direct target of miR-let-7i-5p.

In our study, miR-let-7i-5p mimics resulted in significantly reduced levels of GALE and downstream carcinogenic factors, including N-cad, MMP-2, BCL-2 and CDK4. Moreover, the tumor suppressors bax and p53 were induced after GALE knockdown. These data suggest that miR-let-7i-5p activates GALE signaling during glioma progression. However, it is necessary to further investigate the mechanism by which miR-let-7i-5p regulates the GALE axis in glioma.

In summary, our results confirm the tumor-promoting effect of a new gene, GALE, and its inhibitory miRNA, miR-let-7i-5p, and suggest that GALE may be a prognostic biomarker for high-grade glioma. In addition, GALE is a potential therapeutic target for patients with malignant glioma, especially GBM. One limitation of the current study, however, is the small number of samples included. In addition, the involvement of other key invasion-related proteins has not been studied. Therefore, further research is needed to confirm our findings.

Compliance with Ethical Standards

All applicable international, national, and/or institutional guidelines for the care and use of animals were followed. All procedures performed in studies involving human participants were in accordance with the ethical standards of the institutional and/or national research committee and with the 1964 Helsinki declaration and its later amendments or comparable ethical standards. Informed consent was obtained from all individual participants included in the study. All described procedures involving experimental animals were performed in agreement with the ARRIVE Guidelines and under requirements of the Animal Care and Use Committee of Qilu Hospital of Shandong University.

Author Contributions

All authors contributed to the study conception and design and performed material preparation, and data collection and analysis. The first draft of the manuscript was written by Xiaopeng Sun, and all authors commented on previous versions of the manuscript. All authors made substantial contributions to the conception and design, acquisition of data, or

analysis and interpretation of data; took part in drafting the article or revising it critically for important intellectual content; gave final approval of the version to be published; and agreed to be accountable for all aspects of the work.

Funding

Disclosure

The authors have no potential conflicts of interest to disclose.

References

1. Andratschke N, Grosu AL, Molls M, Nieder C. Perspectives in the treatment of malignant gliomas in adults. *Anticancer Res*. 2001;21 (5):3541–3550.
2. Meyer MA. Malignant gliomas in adults. *N Engl J Med*. 2008;359 (17):1850. author reply 1850.
3. Wen PY, Kesari S. Malignant gliomas in adults. *N Engl J Med*. 2008;359(5):492–507. doi:10.1056/NEJMra0708126
4. Leloir LF. The enzymatic transformation of uridine diphosphate glucose into a galactose derivative. *Arch Biochem Biophys*. 1951;33 (2):186–190. doi:10.1016/0003-9861(51)90096-3
5. Thoden JB, Wohlers TM, Fridovich-Keil JL, et al. Human UDP-galactose 4-epimerase. Accommodation of UDP-N-acetylglucosamine within the active site. *J Biol Chem*. 2001;276(18):15131–15136. doi:10.1074/jbc.M100220200
6. da Silveira Mitteldorf CA, de Sousa-canavez JM, Leite KRM, et al. FN1, GALE, MET, and QPCT overexpression in papillary thyroid carcinoma: molecular analysis using frozen tissue and routine fine-needle aspiration biopsy samples. *Diagn Cytopathol*. 2011;39 (8):556–561. doi:10.1002/dc.v39.8
7. Macfarlane LA, Murphy PR. MicroRNA: biogenesis, function and role in cancer. *Curr Genomics*. 2010;11(7):537–561. doi:10.2174/138920210793175895
8. Liu S, Yin F, Zhang J, et al. Regulatory roles of miRNA in the human neural stem cell transformation to glioma stem cells. *J Cell Biochem*. 2014;115(8):1368–1380. doi:10.1002/jcb.v115.8
9. Zhao Z, Tan X, Zhao A, et al. microRNA-214-mediated UBC9 expression in glioma. *BMB Rep*. 2012;45(11):641–646. doi:10.5483/BMBRep.2012.45.11.097
10. Ma L, Young J, Prabhala H, et al. miR-9, a MYC/MYCN-activated microRNA, regulates E-cadherin and cancer metastasis. *Nat Cell Biol*. 2010;12(3):247–256. doi:10.1038/ncb2024
11. Dews M, Homayouni A, Yu D, et al. Augmentation of tumor angiogenesis by a Myc-activated microRNA cluster. *Nat Genet*. 2006;38 (9):1060–1065. doi:10.1038/ng1855
12. Zhang R, Pang B, Xin T, et al. Plasma miR-221/222 family as novel descriptive and prognostic biomarkers for glioma. *Mol Neurobiol*. 2016;53(3):1452–1460. doi:10.1007/s12035-014-9079-9
13. Gabriely G, Yi M, Narayan RS. et al. Human glioma growth is controlled by microRNA-10b. *Cancer Res*. 2011;71(10):3563–3572. doi:10.1158/0008-5472.CAN-10-3568

14. Boyerinas B, Park SM, Hau A, et al. The role of let-7 in cell differentiation and cancer. *Endocr Relat Cancer*. 2010;17(1):F19–36. doi:10.1677/ERC-09-0184
15. Hertel J, Bartschat S, Wintsche A, Otto C. Evolution of the let-7 microRNA family. *RNA Biol*. 2012;9(3):231–241. doi:10.4161/rna.18974
16. Ali S, Saleh H, Sethi S, et al. MicroRNA profiling of diagnostic needle aspirates from patients with pancreatic cancer. *Br J Cancer*. 2012;107(8):1354–1360. doi:10.1038/bjc.2012.383
17. Akao Y, Nakagawa Y, Naoe T. let-7 microRNA functions as a potential growth suppressor in human colon cancer cells. *Biol Pharm Bull*. 2006;29(5):903–906. doi:10.1248/bpb.29.903
18. Takamizawa J, Konishi H, Yanagisawa K, et al. Reduced expression of the let-7 microRNAs in human lung cancers in association with shortened postoperative survival. *Cancer Res*. 2004;64(11):3753–3756. doi:10.1158/0008-5472.CAN-04-0637
19. Yu F, Yao H, Zhu P, et al. let-7 regulates self renewal and tumorigenicity of breast cancer cells. *Cell*. 2007;131(6):1109–1123. doi:10.1016/j.cell.2007.10.054
20. Hanahan D, Weinberg RA. Hallmarks of cancer: the next generation. *Cell*. 2011;144(5):646–674. doi:10.1016/j.cell.2011.02.013
21. McCorvie TJ, Timson DJ. In silico prediction of the effects of mutations in the human UDP-galactose 4′-epimerase gene: towards a predictive framework for type III galactosemia. *Gene*. 2013;524 (2):95–104. doi:10.1016/j.gene.2013.04.061
22. Schulz JM, Ross KL, Malmstrom K, et al. Mediators of galactose sensitivity in UDP-galactose 4′-epimerase-impaired mammalian cells. *J Biol Chem*. 2005;280(14):13493–13502. doi:10.1074/jbc.M414045200
23. Wasilenko J, Fridovich-Keil JL. Relationship between UDP-galactose 4′-epimerase activity and galactose sensitivity in yeast. *J Biol Chem*. 2006;281(13):8443–8449. doi:10.1074/jbc.M600778200
24. Bang YL, Nguyen TT, Trinh TT, et al. Functional analysis of mutations in UDP-galactose-4-epimerase (GALE) associated with galactosemia in Korean patients using mammalian GALE-null cells. *FEBS J*. 2009;276(7):1952–1961. doi:10.1111/j.1742-4658.2009.06922.x
25. Brahma A, Banerjee N, Bhattacharyya D. UDP-galactose 4-epimerase from Kluyveromyces fragilis–catalytic sites of the homodimeric enzyme are functional and regulated. *FEBS J*. 2009;276(22):6725–6740. doi:10.1111/j.1742-4658.2009.07386.x
26. Brahma A, Bhattacharyya D. UDP-galactose 4-epimerase from Kluyveromyces fragilis: existence of subunit independent functional site. *FEBS Lett*. 2004;577(1–2):27–34. doi:10.1016/j.febslet.2004.09.056
27. Nayar S. UDP-galactose 4-epimerase from Kluyveromyces fragilis: analysis of its hysteretic behavior during catalysis. *Biochemistry*. 2004;43(31):10212–10223. doi:10.1021/bi049569t
28. Pey AL, Padín-Gonzalez E, Mesa-Torres N, Timson DJ. The metastability of human UDP-galactose 4′-epimerase (GALE) is increased by variants associated with type III galactosemia but decreased by substrate and cofactor binding. *Arch Biochem Biophys*. 2014;562:103–114. doi:10.1016/j.abb.2014.07.030
29. Timson DJ. Functional analysis of disease-causing mutations in human UDP-galactose 4-epimerase. *FEBS J*. 2005;272(23):6170–6177. doi:10.1111/j.1742-4658.2005.05017.x
30. Thoden JB, Wohlers TM, Fridovich-Keil JL, et al. Molecular basis for severe epimerase deficiency galactosemia. X-ray structure of the human V94m-substituted UDP-galactose 4-epimerase. *J Biol Chem*. 2001;276(23):20617–20623. doi:10.1074/jbc.M101304200
31. Wohlers TM, Christacos NC, Harreman MT, et al. Identification and characterization of a mutation, in the human UDP-galactose-4-epimerase gene, associated with generalized epimerase-deficiency galactosemia. *Am J Hum Genet*. 1999;64(2):462–470. doi:10.1086/302263
32. Timson DJ. The molecular basis of galactosemia - Past, present and future. *Gene*. 2016;589(2):133–141. doi:10.1016/j.gene.2015.06.077
33. McCorvie TJ, Wasilenko J, Liu Y, et al. In vivo and in vitro function of human UDP-galactose 4′-epimerase variants. *Biochimie*. 2011;93 (10):1747–1754. doi:10.1016/j.biochi.2011.06.009

34. Que T, Song Y, Liu Z, et al. Decreased miRNA-637 is an unfavorable prognosis marker and promotes glioma cell growth, migration and invasion via direct targeting Akt1. *Oncogene*. 2015;34(38):4952–4963. doi:10.1038/onc.2014.419

35. Shi Y, Chen C, Zhang X, et al. Primate-specific miR-663 functions as a tumor suppressor by targeting PIK3CD and predicts the prognosis of human glioblastoma. *Clin Cancer Res*. 2014;20(7):1803–1813. doi:10.1158/1078-0432.CCR-13-2284

36. Tu Y, Gao X, Li G, et al. MicroRNA-218 inhibits glioma invasion, migration, proliferation, and cancer stem-like cell self-renewal by targeting the polycomb group gene Bmi1. *Cancer Res*. 2013;73 (19):6046–6055. doi:10.1158/0008-5472.CAN-13-0358

37. Godlewski J, Nowicki MO, Bronisz A, et al. Targeting of the Bmi-1 oncogene/stem cell renewal factor by microRNA-128 inhibits glioma proliferation and self-renewal. *Cancer Res*. 2008;68(22):9125–9130. doi:10.1158/0008-5472.CAN-08-2629

38. Li Y, Guessous F, Zhang Y, et al. MicroRNA-34a inhibits glioblastoma growth by targeting multiple oncogenes. *Cancer Res*. 2009;69 (19):7569–7576. doi:10.1158/0008-5472.CAN-09-0529